

Probing the relationships between molecular conformation and intermolecular contacts in *N,N*-dibenzyl-*N'*-(furan-2-carbonyl)thiourea

Hiram Pérez,^a Rodrigo S. Corrêa,^b Ana María Plutín,^c
Beatriz O'Reilly^c and Marcelo B. Andrade^{d*}

^aDepartamento de Química Inorgánica, Facultad de Química, Universidad de la Habana, Habana 10400, Cuba, ^bDepartamento de Química, Universidade Federal de São Carlos, CEP 13565-905, São Carlos, SP, Brazil, ^cLaboratório de Síntesis Orgânica, Facultad de Química, Universidad de la Habana, Habana 10400, Cuba, and ^dGrupo de Cristalografía, Instituto de Física de São Carlos, Universidade de São Paulo, CEP 13560-970, São Carlos, Brazil
Correspondence e-mail: mabadean@terra.com.br

Received 11 October 2011

Accepted 6 December 2011

Online 9 December 2011

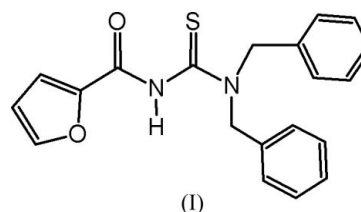
In the crystal structure of the title compound, $C_{20}H_{18}N_2O_2S$, molecules are linked by bifurcated $C-H \cdots O$ hydrogen-bond interactions, giving rise to chains whose links are composed of alternating centrosymmetrically disposed pairs of molecules and characterized by $R_2^2(10)$ and $R_2^2(20)$ hydrogen-bonding motifs. Also, $N-H \cdots S$ hydrogen bonds form infinite zigzag chains along the [010] direction, which exhibit the $C(4)$ motif. Hirshfeld surface and fingerprint plots were used to explore the intermolecular interactions in the crystal structure. This analysis confirms the important role of $C-H \cdots O$ hydrogen bonds in the molecular conformation and in the crystal structure, providing a potentially useful tool for a full understanding of the intermolecular interactions in acylthiourea derivatives.

Comment

In recent years, acylthiourea derivatives have been extensively studied and many biological activities attributed to them, such as pesticidal, fungicidal, antiviral and plant-growth regulatory activities (Hernández *et al.*, 2003). *N*-Acyl-*N',N'*-disubstituted thiourea derivatives have also attracted considerable attention because of their coordination ability with transition metal ions (Binzet *et al.*, 2009). Recently, we have begun to study a novel series of *N*-acyl-*N',N'*-disubstituted thiourea derivatives and their complexes with transition metals (Pérez, Corrêa, Duque *et al.*, 2008; Pérez, Mascarenhas *et al.*, 2008; Pérez, Corrêa, Plutín *et al.*, 2008; Pérez *et al.*, 2009).

One of these derivatives is the title compound, (I) (Fig. 1), and we have investigated its crystal structure in order to study the intra- and intermolecular interactions and their influence on molecular conformation and crystal assembly. The C2—S1

and C1—O1 bonds have lengths indicating double-bond character, whereas the C—N bonds are single (Table 1). The conformation of the molecule with respect to the thiocarbonyl and carbonyl groups is twisted, as reflected by the C1—N1—C2—N2 and S1—C2—N1—C1 torsion angles (Table 1). As the thiourea and acyl units are not coplanar and the bond lengths do not present significant C2—S1 and C1—O1 lengthening or



C—N shortening, resonance effects are absent in this part of the molecule. For related compounds, it has been observed that the resonance effect involving the acylthiourea moiety is only present when there is a proton linked to N2 (Corrêa *et al.*,

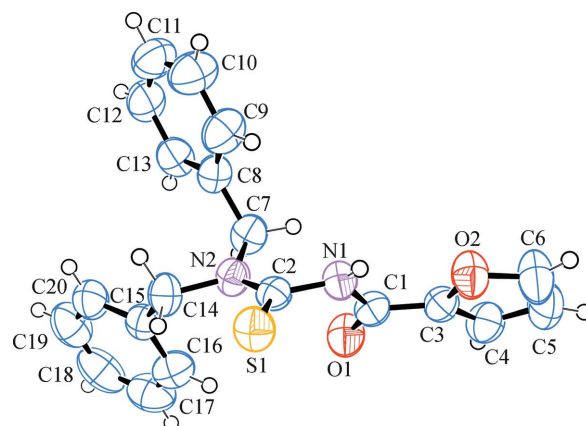


Figure 1
The molecular structure of (I), showing the atom-numbering scheme. Displacement ellipsoids are drawn at the 50% probability level.

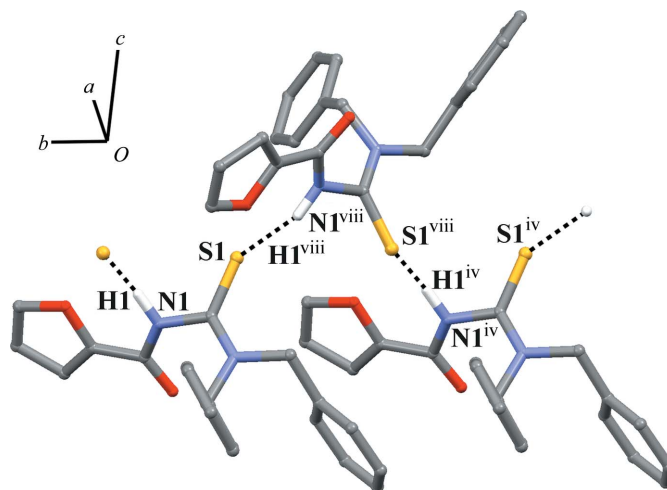


Figure 2
A view of (I), showing intermolecular $N-H \cdots S$ hydrogen bonds (dashed lines) forming an infinite $C(4)$ zigzag chain along the [010] direction. [Symmetry codes: (iv) $x, y - 1, z$; (viii) $-x + 2, y - \frac{1}{2}, -z + \frac{1}{2}$.]

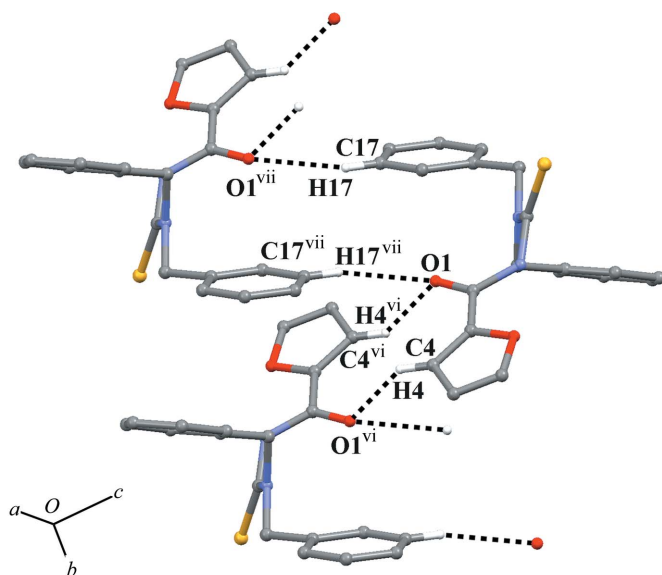


Figure 3

A representation of the molecules of (I) connected by nonclassical C–H...O hydrogen bonding (dashed lines). [Symmetry codes: (vi) $-x + 2, -y + 1, -z$; (vii) $-x + 2, -y, -z$].

2008; Estévez-Hernández *et al.*, 2008). As atom N2 is fully substituted in (I), this effect is not active.

In the crystal structure, molecules of (I) are linked into infinite zigzag chains along [010] by N–H...S hydrogen bonds, giving a $C(4)$ hydrogen-bonding motif (Bernstein *et al.*, 1995; Fig. 2). A search of the Cambridge Structural Database (CSD; Version 5.32, update of November 2011; Allen, 2002) for organic acylthiourea substructures revealed 440 such crystal structures. Some 236 of these structures exhibit a characteristic intermolecular pattern, forming dimers *via* N–H...S hydrogen bonding to give an eight-membered ring exhibiting an $R_2^2(8)$ hydrogen-bonding motif (Shanmuga Sundara Raj *et al.*, 1999; Corrêa *et al.*, 2008; Gomes *et al.*, 2010). An interesting acceptor-bifurcated intermolecular interaction is observed in (I), involving carbonyl atom O1 and forming an H4...O1...H17 angle of 76.3° . In this contact, the 2-furoyl C4–H4 fragment at $(-x + 2, -y + 1, z)$ is linked to atom O1, forming an $R_2^2(10)$ hydrogen-bonding motif (Fig. 3), whereas in the second interaction, atom O1 acts as acceptor from the C17–H17 group at $(-x + 1, -y, -z)$, forming an $R_2^2(20)$ hydrogen-bonding motif (Fig. 3). The latter contact plays a role in establishing and stabilizing the conformation of the C15–C20 ring. In thiourea derivatives, these structural motifs, *viz.* ten- and 20-membered rings mediated by C–H...O hydrogen bonding, are unexpected. Furthermore, there is no indication in (I) of any intermolecular hydrogen bonding between the NH group and the O atom of the furan ring. As a result, the packing in (I) comprises a network of hydrogen bonds and noncovalent contacts (Table 2) forming alternating hydrophilic and hydrophobic regions along the [100] direction (Fig. 4). This pattern of hydrogen bonds is not common in related structures, which prompted us to explore the contributions of the main intermolecular contacts in the crystal packing of (I), as well as the importance of C–H...O

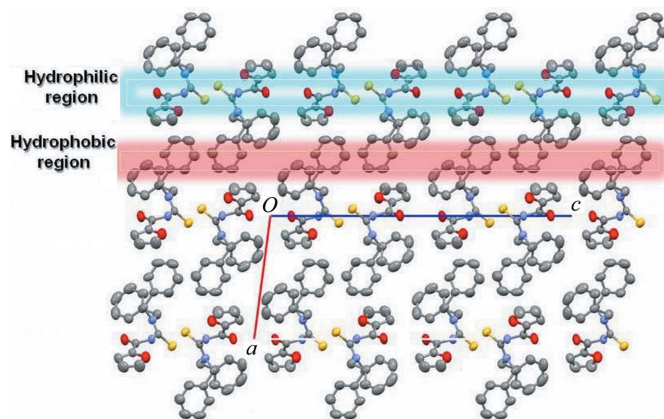


Figure 4

A packing diagram for (I), showing the alternating hydrophilic and hydrophobic regions along the [100] direction.

nonclassical hydrogen bonding in establishing the organization of the extended structure.

Van der Waals interactions (H...H, C...H, S...H, N...H and O...H) are also present in this structure. The main intermolecular interactions in (I) were analysed using the Hirshfeld surface (McKinnon *et al.*, 1998) and the corresponding two-dimensional fingerprint plots (Spackman & Jayatilaka, 2009; McKinnon *et al.*, 2007). Hirshfeld surfaces and their two-dimensional fingerprints are useful tools for visualizing and analysing structural properties in relation to packing patterns. Intermolecular interactions present in the structure of a molecular crystal are depicted by the

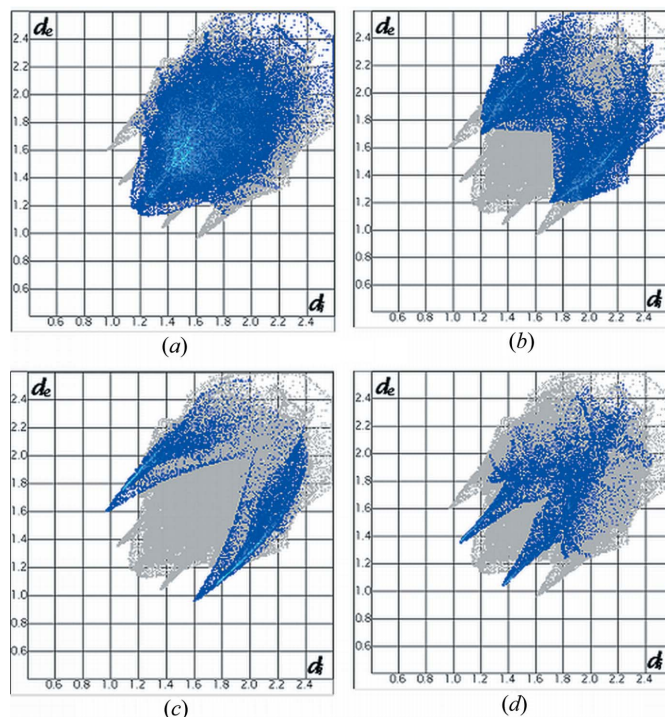


Figure 5

Fingerprint plots of (I) resolved into (a) H...H, (b) C...H, (c) S...H and (d) O...H intermolecular contacts. The full fingerprint appears beneath each decomposed plot as a grey shadow.

construction of the two-dimensional fingerprint graphic, which is a frequency plot of (d_e , d_i) pairs, in which d_e is the distance from a point on the Hirshfeld surface to the nearest external atom and d_i is the distance from the same point on the Hirshfeld surface to the nearest atom internal to the surface. The relative frequency of occurrence of a (d_e , d_i) pair, represented by colours in the fingerprint plot, is an indication of the importance of a particular type of interaction in the crystal structure being examined. As described by Spackman & Jayatilaka (2009), different types of common noncovalent interactions give characteristic patterns in the fingerprint plots. In the two-dimensional diagrams depicted for (I) in Fig. 5, we can identify and compare the types of intermolecular interactions present. Fig. 5(a) isolates H \cdots H contacts and shows spikes centred near a ($d_e + d_i$) sum of 2.4 Å [H6 \cdots H12ⁱ = 2.49 Å; symmetry code: (i) $x + 1, y + 1, z$], whereas Fig. 5(b), isolating C \cdots H contacts, shows spikes centred around ($d_e + d_i$) of 2.9 Å [C1 \cdots H12ⁱⁱ, C12 \cdots H6ⁱⁱⁱ and C19 \cdots H7B^{iv} are 3.03, 2.99 and 3.09 Å, respectively; symmetry codes: (ii) $x + 1, y, z$; (iii) $x - 1, y - 1, z$; (iv) $x, y - 1, z$]. In addition, Figs. 5(c) and 5(d) (S \cdots H and O \cdots H, respectively) show much sharper spikes, revealing specific N—H \cdots S and C—H \cdots O hydrogen bonds with spikes centred around ($d_e + d_i$) sums of 2.6 and 2.4 Å, respectively. These two values indicate that the C—H \cdots O hydrogen bond is the stronger interaction. The relative contributions to the Hirshfeld surface area due to H \cdots H, C \cdots H, S \cdots H, O \cdots H and N \cdots H contacts for (I) are 49.2, 23.4, 12.6, 11.4 and 0.3%, respectively. For the intermolecular contacts, the smallest fingerprint contributions occur for O \cdots S (0.5%) and C \cdots S (0.1%). Also, it is clear that the presence of a network of nonclassical C—H \cdots O contacts exerts an important influence on the stabilization of the packing in (I).

The results reported here underline the utility of Hirshfeld surfaces and fingerprint-plot analysis for a full understanding of the intermolecular contacts in acylthiourea derivatives.

Experimental

The title compound was prepared using the standard procedure previously reported in the literature (Nagasawa & Mitsunobu, 1981) by the reaction of fuoyl chloride with KSCN in anhydrous acetone, and then condensation with dibenzylamine. The reaction mixture was poured into cold water, resulting in precipitation of the solid product. Recrystallization from acetone–water solution (1:1 v/v) yielded colourless crystals of (I) (2.7 g, 9.0 mmol, 90%; m.p. 419 K). IR (KBr, ν , cm^{-1}): 3320 (free NH), 3200 (assoc. NH), 1693 (CO), 1608 (arom.), 1580 (thioureido I), 1425 II, 1173 III, 1025 (C5—O—C8), 928 IV; ¹H NMR (CDCl₃): δ 8.71 (1H, s, broad NH), 7.63 (1H, s, H8, $J = 2.1$ Hz), 7.52–7.32 (10H, m, Ph), 7.10 (1H, s, H6, $J = 3.2$ Hz), 6.60–6.50 (1H, m, H7), 5.20 (2H, s, CH₂), 4.72 (2H, s, CH₂); ¹³C NMR (CDCl₃): δ 189.8 (CS), 153.9 (CO), 147.6 (C5), 145.5 (C8), 138.4 (1 C—Ph), 136.9 (1 C—Ph), 129.1 (2 C—Ph), 128.8 (2 C—Ph), 128.5 (3 C—Ph), 128.4 (3 C—Ph), 127.7 (4 C—Ph), 127.5 (4 C—Ph), 117.6 (C6), 112.9 (C7), 56.1 (CH₂), 55.3 (CH₂). EI–MS (m/e): 350 (20), 95 (100), 91 (84), 65 (31), 39 (6). Analysis calculated for C₂₀H₁₈N₂O₂S: C 68.55, H 5.17, N 7.95, S 9.15%; found: C 68.12, H 5.14, N 8.15, S 9.19%.

Table 1
Selected geometric parameters (Å, °).

C1—O1	1.2147 (19)	C2—S1	1.6614 (16)
C1—N1	1.373 (2)	C7—N2	1.479 (2)
C2—N2	1.332 (2)	C14—N2	1.470 (2)
C2—N1	1.412 (2)		
N2—C2—N1—C1	−64.7 (2)	S1—C2—N1—C1	116.05 (15)

Table 2
Hydrogen-bond geometry (Å, °).

D—H \cdots A	D—H	H \cdots A	D \cdots A	D—H \cdots A
N1—H1 \cdots S1 ^v	0.94	2.60	3.322 (2)	134
C4—H4 \cdots O1 ^{vi}	0.93	2.53	3.325 (2)	143
C17—H17 \cdots O1 ^{vii}	0.93	2.58	3.496 (3)	167

Symmetry codes: (v) $-x + 2, y + \frac{1}{2}, -z + \frac{1}{2}$; (vi) $-x + 2, -y + 1, -z$; (vii) $-x + 2, -y, -z$.

Crystal data

C ₂₀ H ₁₈ N ₂ O ₂ S	$V = 1834.72$ (6) Å ³
$M_r = 350.42$	$Z = 4$
Monoclinic, $P2_1/c$	Mo $K\alpha$ radiation
$a = 10.0449$ (2) Å	$\mu = 0.19$ mm ^{−1}
$b = 7.5527$ (1) Å	$T = 294$ K
$c = 24.3945$ (5) Å	$0.23 \times 0.21 \times 0.09$ mm
$\beta = 97.538$ (1)°	

Data collection

Nonius KappaCCD diffractometer	11569 measured reflections
Absorption correction: Gaussian (based on crystal morphology; Coppens <i>et al.</i> , 1965)	4061 independent reflections
$T_{\min} = 0.959, T_{\max} = 0.983$	2616 reflections with $I > 2\sigma(I)$
	$R_{\text{int}} = 0.038$

Refinement

$R[F^2 > 2\sigma(F^2)] = 0.045$	226 parameters
$wR(F^2) = 0.124$	H-atom parameters constrained
$S = 1.04$	$\Delta\rho_{\text{max}} = 0.13$ e Å ^{−3}
4061 reflections	$\Delta\rho_{\text{min}} = -0.21$ e Å ^{−3}

H atoms were treated as riding, with aromatic C—H = 0.93 Å and methylene C—H = 0.97 Å, and with $U_{\text{iso}}(\text{H}) = 1.2U_{\text{eq}}(\text{C})$. The N-bound H atom was located by difference Fourier synthesis and its position was fixed as initially found, with $U_{\text{iso}}(\text{H}) = 1.2U_{\text{eq}}(\text{N})$.

Data collection: COLLECT (Enraf–Nonius, 2000); cell refinement: SCALEPACK (Otwinowski & Minor, 1997); data reduction: DENZO (Otwinowski & Minor, 1997) and SCALEPACK; program(s) used to solve structure: SHELXS97 (Sheldrick, 2008); program(s) used to refine structure: SHELXL97 (Sheldrick, 2008); molecular graphics: ORTEP-3 for Windows (Farrugia, 1997), Mercury (Macrae *et al.*, 2008) and CrystalExplorer (Wolff *et al.*, 2005); software used to prepare material for publication: WinGX (Farrugia, 1999).

The authors thank the Grupo de Cristalografia, IFSC, USP, Brazil, for allowing the X-ray data collection, and Professor Javier Ellena for useful discussions. The authors acknowledge financial support from the PhD Cooperative Programme ICTP/CLAF. RSC thanks FAPESP for a fellowship (grant No. 2009/08131-1).

Supplementary data for this paper are available from the IUCr electronic archives (Reference: FA3263). Services for accessing these data are described at the back of the journal.

References

- Allen, F. H. (2002). *Acta Cryst.* **B58**, 380–388.
- Bernstein, J., Davis, R. E., Shimoni, I. & Chang, N.-L. (1995). *Angew. Chem. Int. Ed. Engl.* **34**, 1555–1573.
- Binzet, G., Külcü, N., Flörke, U. & Arslan, H. (2009). *J. Coord. Chem.* **62**, 3454–3462.
- Coppens, P., Leiserowitz, L. & Rabinovich, D. (1965). *Acta Cryst.* **18**, 1035–1038.
- Corrêa, R. S., Estévez-Hernández, O., Ellena, J. & Duque, J. (2008). *Acta Cryst.* **E64**, o1414.
- Enraf–Nonius (2000). *COLLECT*. Enraf–Nonius BV, Delft, The Netherlands.
- Estévez-Hernández, O., Duque, J., Ellena, J. & Corrêa, R. S. (2008). *Acta Cryst.* **E64**, o1157.
- Farrugia, L. J. (1997). *J. Appl. Cryst.* **30**, 565.
- Farrugia, L. J. (1999). *J. Appl. Cryst.* **32**, 837–838.
- Gomes, L. R., Santos, L. M. N. B. F., Coutinho, J. P., Schröder, B. & Low, J. N. (2010). *Acta Cryst.* **E66**, o870.
- Hernández, W., Spodine, E., Muñoz, J. C., Beyer, L., Schröder, U., Ferreira, J. & Pavani, M. (2003). *Bioinorg. Chem. Appl.* **1**, 271–284.
- Macrae, C. F., Bruno, I. J., Chisholm, J. A., Edgington, P. R., McCabe, P., Pidcock, E., Rodriguez-Monge, L., Taylor, R., van de Streek, J. & Wood, P. A. (2008). *J. Appl. Cryst.* **41**, 466–470.
- McKinnon, J. J., Jayatilaka, D. & Spackman, M. A. (2007). *Chem. Commun.* **37**, 3814–3816.
- McKinnon, J. J., Mitchell, A. S. & Spackman, M. A. (1998). *Chem. Eur. J.* **4**, 2136–2141.
- Nagasawa, H. & Mitsunobu, O. (1981). *Bull. Chem. Soc. Jpn*, **54**, 2223–2224.
- Otwinowski, Z. & Minor, W. (1997). *Methods in Enzymology*, Vol. 276, *Macromolecular Crystallography*, Part A, edited by C. W. Carter Jr & R. M. Sweet, pp. 307–326. New York: Academic Press.
- Pérez, H., Corrêa, R. S., Duque, J., Plutín, A. M. & O'Reilly, B. (2008). *Acta Cryst.* **E64**, m916.
- Pérez, H., Corrêa, R. S., Plutín, A. M., Calderón, O. & Duque, J. (2009). *Acta Cryst.* **E65**, m242.
- Pérez, H., Corrêa, R. S., Plutín, A. M., O'Reilly, B. & Duque, J. (2008). *Acta Cryst.* **E64**, m733–m734.
- Pérez, H., Mascarenhas, Y., Plutín, A. M., de Souza Corrêa, R. & Duque, J. (2008). *Acta Cryst.* **E64**, m503.
- Shanmuga Sundara Raj, S., Puviarasan, K., Velmurugan, D., Jayanthi, G. & Fun, H.-K. (1999). *Acta Cryst.* **C55**, 1318–1320.
- Sheldrick, G. M. (2008). *Acta Cryst.* **A64**, 112–122.
- Spackman, M. A. & Jayatilaka, D. (2009). *CrystEngComm*, **11**, 19–32.
- Wolff, S. K., Grimwood, D., McKinnon, J., Jayatilaka, D. & Spackman, M. A. (2005). *CrystalExplorer*. Version 2.1 (381). University of Western Australia, Australia.